J. Biochem. 121, 161-171 (1997)

Paracoccus denitrificans Aromatic Amino Acid Aminotransferase: A Model Enzyme for the Study of Dual Substrate Recognition Mechanism[1]

Shinya Oue,* Akihiro Okamoto,* Yumi Nakai,* Masakiyo Nakahira,* Takeji Shibatani,† Hideyuki Hayashi,* and Hiroyuki Kagamiyama*,[2]

*Department of Biochemistry, Osaka Medical College, 2-7 Daigakumachi, Takatsuki, Osaka 569; and †Research Laboratory of Applied Biochemistry, Tanabe Seiyaku Co. Ltd., 16-89 Kashima-3-chome, Yodogawa-ku, Osaka 532

Received for publication, September 24, 1996

The gene for aromatic amino acid aminotransferase (ArAT) from *Paracoccus denitrificans* was cloned, sequenced, and overexpressed in *Escherichia coli* cells. The sequence differed from that reported previously [Takagi, T., Taniguchi, T., Yamamoto, Y., and Shibatani, T. (1991) *Biotechnol. Appl. Biochem.* 13, 112-119]. The enzyme (pdArAT) was purified to homogeneity, and characterized. It was similar to aspartate aminotransferase (AspAT) and ArAT of *E. coli* (ecArAT) in many respects, including gross protein structure and spectroscopic properties. pdArAT showed activities toward both dicarboxylic and aromatic substrates, and analysis of the binding of substrate analogs and quasisubstrates to the enzyme showed that both dicarboxylic and aromatic substrates take a similar orientation in the active site of pdArAT; these properties are essentially identical with those of ecArAT. As in the case of ecArAT, neutral amino acids with larger side chains are better substrates for pdArAT, suggesting that hydrophobic interaction between the substrate and the enzyme is important for the recognition of substrates with neutral side chains. pdArAT catalyzed transamination of phenylalanine and tyrosine far more efficiently (10^2-fold in terms of k_{cat}/K_m) than those of straight-chain aliphatic amino acids with similar side-chain surface area, whereas ecArAT did not show significant preference for aromatic amino acids over aliphatic amino acids. This shows that the substrate-side-chain-binding pocket of pdArAT, as compared with the pocket of ecArAT, is well suited in shape for interaction with the phenyl and hydroxyphenyl rings of substrates. Thus, pdArAT is an ideal enzyme among ArATs for the study of the high-specificity recognition of two different kinds of substrates, the one having a carboxylic side chain and the other having an aromatic side chain.

Key words: aromatic amino acid aminotransferase, aspartate aminotransferase, *Paracoccus denitrificans*, pyridoxal 5′-phosphate, substrate specificity.

Aromatic amino acid aminotransferase (ArAT; EC 2.6.1.57) is a pyridoxal 5′-phosphate (PLP)-dependent enzyme which catalyzes the following reversible transamination reactions,

$$E_L + \text{phenylalanine} \rightleftharpoons E_M + \text{3-phenylpyruvate} \quad (1)$$

$$E_L + \text{tyrosine} \rightleftharpoons E_M + \text{3-(4-hydroxyphenyl)-pyruvate} \quad (2)$$

$$E_L + \text{tryptophan} \rightleftharpoons E_M + \text{3-indolylpyruvate} \quad (3)$$

$$E_L + \text{aspartate} \rightleftharpoons E_M + \text{oxalacetate} \quad (4)$$

$$E_L + \text{glutamate} \rightleftharpoons E_M + \text{2-oxoglutarate} \quad (5)$$

where E_L and E_M denote the PLP-form and the pyridoxamine 5′-phosphate (PMP)-form of the enzyme, respectively. The enzyme in *Escherichia coli* (ecArAT) shows 42% amino acid sequence homology with the *E. coli* aspartate aminotransferase (ecAspAT) and lesser homologies with animal AspATs (*2, 3*). The active-site residues of AspATs which had been identified by X-ray crystallographic studies (*4-6*), were found to be conserved in the primary structure of ecArAT at the corresponding positions (*2, 3*). Both ecArAT and AspATs are composed of two identical subunits of about 43K and contain one PLP molecule per subunit. The absorption and circular dichroism spectra and their pH dependency were essentially identical for the two enzymes (*7*). ecArAT reacts with dicarboxylic amino and oxo acids [reactions (4) and (5)] as efficiently as AspAT, an enzyme catalyzing predominantly reactions (4) and (5) (*7-9*). Thus ecArAT is capable of recognizing two structurally different sets of substrates, one having an aromatic side chain and the other having an

[1] This work was supported by Grants-in-Aid (No. 03780187 to H.H. and 14454160 to H.K.) from the Ministry of Education, Science, Sports and Culture of Japan, and by the Research Grant from Japan Society for the Promotion of Science (Research for the Future). The nucleotide sequence of the pdArAT gene has been deposited in the EMBL nucleotide sequence database under the accession number Y08272.

[2] To whom correspondence should be addressed. Phone: +81-726-83-1221 (Ext. 2644), Fax: +81-726-84-6516

Abbreviations: ArAT, aromatic amino acid aminotransferase [EC 2.6.1.57]; AspAT, aspartate aminotransferase [EC 2.6.1.1]; HEPES, *N*-(2-hydroxyethyl)piperazine-*N*′-(2-ethanesulfonic acid); K-P_i, potassium phosphate buffer; PIPES, piperazine-*N*,*N*′-bis(2-ethanesulfonic acid); PLP, pyridoxal 5′-phosphate; PMP, pyridoxamine 5′-phosphate.

acidic side chain. A number of analyses have been carried out for the purpose of understanding this characteristic feature of substrate recognition of ecArAT (*7, 10, 11*). Spectroscopic studies using β-hydroxylated substrates and [Tyr70→Phe] mutant enzyme indicated that the aromatic ring of the substrate phenylalanine occupies the same region as that occupied by the β-carboxyl group of the substrate aspartate, by demonstrating the interaction between the hydroxy group of the quasisubstrates and the hydroxy group of Tyr70 (*7, 10*). This suggested a substrate-recognition mechanism in which Arg292,*[3] the residue that binds the β-carboxylate group of dicarboxylic substrates, switches its position in the recognition of aromatic side chains. This mechanism for the dual substrate recognition has also been found in the crystal structure of the phenylpropionate complex of a hexamutant AspAT, which mimics ecArAT owing to the replacement of six residues located near the active site with those of ecArAT in order to increase the hydrophobicity of the active site, and has increased activity toward aromatic amino acids without loss of AspAT activity (*11*). However, X-ray crystallographic analysis on ecArAT itself, which would provide important findings on the enzyme-substrate interactions and the dual substrate-recognition mechanism, has not been carried out, because the crystallization of the enzyme has been unsuccessful. Therefore, we planned to change the source of the enzyme for crystallization. Our choices were ArAT from *Salmonella typhimurium* (*12*) and ArAT from *Paracoccus denitrificans* (*13*, this study). The *Salmonella* enzyme has not been crystallized yet. On the other hand, we were able to obtain a good crystal of *P. denitrificans* ArAT (Okamoto *et al.*, manuscript in preparation). As a first step for detailed structural and functional analysis of the *Paracoccus* ArAT (pdArAT), we expressed the enzyme in *E. coli*, and physicochemically characterized the expressed protein.

MATERIALS AND METHODS

Chemicals—3-(4-Hydroxyphenyl)propionic acid (fluorometric grade) was obtained from Nacalai Tesque (Kyoto). 3-Phenylpropionic acid and 3-indolepropionic acid were recrystallized twice from petroleum ether and chloroform, respectively, before use. 3-Indolepyruvic acid, 3-phenylpyruvic acid, 3-(4-hydroxyphenyl)pyruvic acid, DL-*threo*-3-hydroxyaspartic acid, and DL-*threo*-3-phenylserine were obtained from Sigma (St. Louis, MO). L-*Erythro*-3-phenylserine was synthesized as described by Jones (*14*). L-*Erythro*-3-hydroxyaspartic acid was synthesized by the method of Jenkins (*15*). DL-2-Aminoheptanoic acid was synthesized by the method of Albertson (*16*). *E. coli* ArAT (*7*) and AspAT (*17*) were prepared as described previously. All other chemicals were of the highest grade commercially available.

Amplification of the pdArAT Gene—Genomic DNA was obtained from *P. denitrificans* IFO12442 cells by a standard method (*18*). Primer oligonucleotides, the sequences of which were AAACCCGTCATCACCACTGCGGCT (forward) and ACGTGGAAGAAAAAGGCGCGTCT (reverse), were designed based on the published sequence of the pdArAT gene (*13*), to amplify a DNA fragment containing the coding and the promoter regions. Polymerase chain reaction was carried out using 0.5 μg of genomic DNA. The amplified DNA was recovered from the agarose gel after electrophoresis using GeneClean II (BIO 101, Vista, CA), and was ligated to a TA vector pCR™II (Invitrogen, San Diego, CA). The DNA fragment containing the pdArAT gene was subcloned into pUC118 just downstream of the *lac* promoter, in order to express the pdArAT protein (see the legend to Fig. 1).

Assay of Enzyme Activity—In the purification steps, the ArAT activity was measured according to the method of Inoue *et al.* (*19*). The assay mixture contained, in 2 ml, 0.1 M Tris-HCl, pH 8.0, 5 mM L-tryptophan, 20 mM 2-oxoglutarate, 5 μM pyridoxal 5′-phosphate (PLP), and the enzyme. The reaction was started by the addition of the enzyme, and the formation of the product, 3-indolepyruvate, was monitored at 310 nm. The rate of the reaction was calculated using a value of 3,180 $M^{-1} \cdot cm^{-1}$ for the difference of the molar absorptivity of 3-indolepyruvate and 2-oxoglutarate at 310 nm (*19*).

Purification of the Enzyme—E. coli TY103 (*20*) cells (50 g) harboring the pdArAT overexpression plasmid were sonicated in 100 ml of 20 mM potassium phosphate (K-P_i), containing 10 mM 2-oxoglutarate, 5 mM 2-mercaptoethanol, 10 μM PLP, pH 7.0. Fifty microliters of the buffer was added, and the lysate was centrifuged at 10,000 × *g* for 30 min. To the supernatant, solid ammonium sulfate was added to a final concentration of 40% saturation. The solution was left on ice for 30 min, and was centrifuged as above. The supernatant was applied to a Phenyl-Toyopearl 650M (Tosoh, Tokyo) column (200 ml bed volume) equilibrated with buffer A (20 mM K-P_i, 10 mM succinate, 5 mM 2-mercaptoethanol, 10 μM PLP, 40% ammonium sulfate, pH 7.0). The column was washed with 250 ml of buffer A, and the proteins were eluted by a linear gradient formed between 500 g of buffer A and 500 g of buffer B (2 mM K-P_i, 10 mM succinate, 5 mM 2-mercaptoethanol, 10 μM PLP, pH 7.0). The active, yellow fractions were collected, concentrated to 50 ml, and dialyzed against buffer B. The dialysate was applied to a hydroxyapatite (Bio-Rad, Hercules, CA) column (100 ml bed volume) equilibrated with buffer B, washed with 100 ml of buffer B, and the enzyme was eluted by a linear gradient formed between 500 g of buffer B and 500 g of 100 mM K-P_i, 10 mM succinate, and 5 mM 2-mercaptoethanol, pH 7.0. The fractions were analyzed by SDS-PAGE, and the high-purity fractions were collected, and concentrated to about 10 ml. This solution was applied to a Sephacryl S-200 (Pharmacia, Uppsala, Sweden) column (30 mm × 800 mm) equilibrated with 20 mM K-P_i, 10 mM succinate, 5 mM 2-mercaptoethanol, 5 μM PLP, and 0.1 M KCl, pH 7.0. The final preparation was >97% pure as judged by SDS-PAGE. The purified enzyme was concentrated to about 10 mg/ml, sterilized by filtration, and stored at 4°C before use.

Preparation of the Pyridoxamine 5′-Phosphate (PMP)-Form Enzyme—pdArAT was isolated in the PLP form. To obtain the PMP-form enzyme, the PLP-form pdArAT was incubated with 50 mM L-cysteinesulfinate for 10 min at 25°C in 50 mM HEPES-NaOH buffer, pH 7.0, containing 10 μM PMP. The enzyme was then passed through a PD-10

[3] Amino acid residues are numbered according to the sequence of pig cytosolic aspartate aminotransferase (*1*). An asterisk (*) indicates that the residue comes from the neighboring subunit of the homodimer.

column (Pharmacia, Uppsala, Sweden) equilibrated with 50 mM HEPES-NaOH buffer, pH 7.0, to yield the PMP-form ArAT. The PMP-form ArAT thus obtained had the same specific activity as the PLP-form ArAT when they were assayed in the absence of coenzymes in the assay mixture.

Determination of Kinetic Parameters—The rate of the steady-state transamination reaction with aspartate and 2-oxo acids as substrates was measured using malate dehydrogenase (MDH)-coupling assay in which the oxidation of $NADH^+$ by oxalacetate was monitored at 340 nm (*21*). Each 2 ml reaction mixture contained 50 mM HEPES-NaOH, pH 8.0, 0.1 M KCl, 0.15 mM NADH, 0.025 mg/ml MDH, 0.05-50 mM L-aspartate, and 0.005-20 mM of a 2-oxo acid.

Rapid reactions were followed on an Applied Photophysics SX.17MV stopped-flow spectrophotometer. The dead time for this system was 2.0 ms under a pressure of 500 kPa. The reactions of the PLP form of pdArAT with amino acids were observed to proceed in a monophasic manner. At a fixed substrate concentration the value of the apparent rate constant (k_{app}) was independent of the wavelength used to follow the reaction. The k_{app} values for several different substrate concentrations were obtained by monitoring the reaction at 356 nm. The k_{app} value was found to be dependent on the substrate concentration, as shown by the following equation

$$k_{app} = \frac{k_{cat,Am}^{half}[S]}{K_{m,Am}^{half} + [S]} + \frac{2k_{cat,Ox}^{half}[P]}{K_{m,Ox}^{half} + [P]} \quad (6)$$

where K_m^{half} and k_{cat}^{half} are the K_m and k_{cat} values for the half transamination reaction (see Eqs. 1-5), and [S] and [P] are the concentration of the amino acid and oxo acid, respectively (*17*). Subscripts Am and Ox indicate that the value is for the amino acid substrate and the oxo acid substrate, respectively. The k_{app} values for the reactions of pdArAT with aspartate, phenylalanine, tyrosine, and tryptophan were significantly affected by the contributions of the reverse reactions of the PMP-form ArAT with the corresponding oxo acids (Eq. 6, second term). The rates of these reverse reactions were estimated from the K_m^{half} and k_{cat}^{half} values for the oxo acids, and were subtracted from the k_{app} values according to the method described for the reaction of AspAT with aspartate (*17*). The reactions of pdArAT with other amino acids had high K_m^{half} values, and the k_{app} values were obtained at high amino acid concentrations. Hence the enzyme was mostly converted to the PMP form. In such cases, Eq. 6 is simplified to

$$k_{app} = \frac{k_{cat,Am}^{half}[S]}{K_{m,Am}^{half} + [S]} + 2k_{cat,Ox}^{half} \quad (7)$$

and the K_m^{half} and k_{cat}^{half} values for amino acids were obtained.

Determination of Protein Concentration—The concentration of ArAT subunit in solution was determined spectrophotometrically. The apparent molar extinction coefficients used were $\varepsilon_M = 3.11 \times 10^4\ M^{-1} \cdot cm^{-1}$ for the PLP-form enzyme and $\varepsilon_M = 3.01 \times 10^4\ M^{-1} \cdot cm^{-1}$ for the PMP-form enzyme at 280 nm. These values were calculated based upon the molar absorptivity values of tryptophan and tyrosine as described previously (*17*).

Spectrophotometric Measurements—Absorption spectra were measured using a Hitachi spectrophotometer U-3300. The buffer solution for the absorption measurements contained 50 mM PIPES-NaOH, 50 mM HEPES-NaOH, or 50 mM sodium borate as buffer component(s), and 0.1 M KCl. Protein concentrations were generally $1\text{-}2 \times 10^{-5}$ M.

RESULTS AND DISCUSSION

Cloning, Sequencing, and Overexpression of the pdArAT Gene and Purification of the pdArAT Protein—The PCR product of the *P. denitrificans* genomic DNA using oligonucleotide primers flanking the promoter and the coding region was ligated to a TA vector. Transformation of *E. coli* JM109 cells with the plasmid DNA gave 4 colonies. Sequencing of the entire insert region of the 4 clones showed that 3 of the clones were identical, and the remaining 1 clone contained a single base replacement (ATC to GTC) corresponding to the [Ile262→Val] replacement of the pdArAT protein. We considered that this base replacement was due to a misincorporation of a base during PCR, and, therefore, we used the identical 3 clones for the following experiments. The entire nucleotide and deduced amino acid sequences of the identical 3 clones are shown in Fig. 1. The nucleotide sequence was very similar, but not identical, to that reported by Takagi *et al.* (*13*). The sequence we have determined had 12 insertions and 5 deletions. In addition, 6 bases were unmatched between the two sequences. As a result, in the deduced amino acid sequence of Fig. 1, there were a deletion of an isoleucine residue just before Met359, 18 residues attached at the C-terminal, and extensive alterations of the sequence between residues 116 and 123, and between residues 313 and 338, as compared with the sequence of Takagi *et al.* (*13*). One possible reason for these discrepancies is that the gene we obtained is homologous to but distinct from the gene that had been obtained previously. However, considering the almost identical nucleotide sequences of the 5′- and 3′-untranslated regions between the two pdArAT gene sequences, we think this is unlikely. When being aligned with the amino acid sequences of ecArAT and ecAspAT (Fig. 2), the amino acid sequence we have determined showed fewer insertions and deletions than the sequence of Takagi *et al.* (*13*). The amino acid sequence of the latter from residue 310 to 356 has been suggested to be erroneous because of its low similarity to those of other aminotransferases related to AspAT (*22*). The sequence we have determined could be well aligned in this region with ecAspAT and ecArAT. Transformation of the *E. coli* TY103 cells, deficient in AspAT and ecArAT (*20*), with pUC118 containing the pdArAT gene in its *Eco*RI site downstream of the *lac* promoter, resulted in an overexpression of a protein with M_r of 43,000, as judged by SDS-PAGE (data not shown). The purification of the recombinant pdArAT, expressed in *E. coli*, was performed by sequential hydrophobic, hydroxyapatite, ion-exchange, and size-exclusion chromatographic procedures (see "MATERIALS AND METHODS"). In all chromatographic steps, the ArAT activity eluted as a single peak with an intense yellow color which comes from the PLP molecule attached to the enzyme protein. The final preparation was homogeneous as judged from SDS-PAGE. Generally, 80-120 mg pure enzyme protein was obtained from 30 g wet weight of transformed *E. coli* cells. The purified pdArAT showed a single peak with $m/z = 42{,}653$ on JEOL (Tokyo) JMS-LD11700 TOF mass spectrometry. This size of the subunit

```
                                                    AAACCCGTCATCACCACTGCGGCTCGGGGGTGACGGCGGCCGTGCTGTTCCTGGCGCTTGAACG
                                                    F
CATCGGGCACCGGGACCATTCGCTTTATGACGGAAGCTGGGCCGAATGGGGCAGGTTCCCCGACCTTAAAATCGCAACCGGAGACGCGTG

        10         20         30         40         50         60         70         80         90
ATGCTGGGCAATCTGAAACCGCAGGCCCCCGACAAGATCCTGGCCCTGATGGGCGAATTCAGGGCCGATCCCCGCCAGGGCAAGATCGAC
M  L  G  N  L  K  P  Q  A  P  D  K  I  L  A  L  M  G  E  F  R  A  D  P  R  Q  G  K  I  D
1                          10                         20                         30

       100        110        120        130        140        150        160        170        180
CTGGGCGTGGGGGTCTACAAGGATGCCACCGGCCACACCCCGATCATGCGGGCCGTCCACGCCGCCGAGCAGCGCATGCTGGAAACCGAG
L  G  V  G  V  Y  K  D  A  T  G  H  T  P  I  M  R  A  V  H  A  A  E  Q  R  M  L  E  T  E
                           40                         50                         60

       190        200        210        220        230        240        250        260        270
ACCACCAAGACCTATGCCGGCCTCTCGGGCGAGCCCGAGTTCCAAAAGGCCATGGGCGAGCTGATCCTGGGCGACGGACTGAAATCCGAG
T  T  K  T  Y  A  G  L  S  G  E  P  E  F  Q  K  A  M  G  E  L  I  L  G  D  G  L  K  S  E
                           70                         80                         90

       280        290        300        310        320        330        340        350        360
ACCACCGCGACGCTGGCGACGGTCGGCGGCACCGGCGCCCTCCGGCAGGCGCTGGAACTGGCGCGCATGGCGAACCCGGACCTGCGGGTC
T  T  A  T  L  A  T  V  G  G  T  G  A  L  R  Q  A  L  E  L  A  R  M  A  N  P  D  L  R  V
                          100                        110                        120

       370        380        390        400        410        420        430        440        450
TTCGTCAGCGATCCGACCTGGCCGAACCATGTCTCGATCATGAATTTCATGGGCCTGCCGGTGCAGACCTATCGCTATTTCGATGCCGAG
F  V  S  D  P  T  W  P  N  H  V  S  I  M  N  F  M  G  L  P  V  Q  T  Y  R  Y  F  D  A  E
                          130                        140                        150

       460        470        480        490        500        510        520        530        540
ACCCGCGGCGTCGATTTCGAGGGCATGAAGGCCGACCTCGCCGCCGCGAAAAAGGGCGACATGGTGCTGCTGCACGGCTGCTGCCACAAC
T  R  G  V  D  F  E  G  M  K  A  D  L  A  A  A  K  K  G  D  M  V  L  L  H  G  C  C  H  N
                          160                        170                        180

       550        560        570        580        590        600        610        620        630
CCGACCGGCGCCAACCTGACGCTGGATCAATGGGCCGAGATCGCCTCGATCCTGGAAAAGACCGGCGCGCTGCCGCTGATCGACCTGGCC
P  T  G  A  N  L  T  L  D  Q  W  A  E  I  A  S  I  L  E  K  T  G  A  L  P  L  I  D  L  A
                          190                        200                        210

       640        650        660        670        680        690        700        710        720
TATCAGGGCTTCGGCGACGGGCTGGAAGAGGACGCGGCCGGCACCCGGCTGATCGCCTCGCGCATCCCCGAGGTGCTGATCGCGGCCTCG
Y  Q  G  F  G  D  G  L  E  E  D  A  A  G  T  R  L  I  A  S  R  I  P  E  V  L  I  A  A  S
                          220                        230                        240

       730        740        750        760        770        780        790        800        810
TGCAGCAAGAACTTCGGCATCTACCGCGAACGCACCGGCTGCCTGCTGGCGCTTTGCGCCGATGCGGCGACCAGGGAGCTGGCGCAGGGC
C  S  K  N  F  G  I  Y  R  E  R  T  G  C  L  L  A  L  C  A  D  A  A  T  R  E  L  A  Q  G
                          250                        260                        270

       820        830        840        850        860        870        880        890        900
GCCATGGCCTTCCTGAACCGCCAGACCTATTCCTTCCCGCCCTTCCACGGCGCCAAGATCGTCTCGACCGTGCTGACCACGCCCGAACTG
A  M  A  F  L  N  R  Q  T  Y  S  F  P  P  F  H  G  A  K  I  V  S  T  V  L  T  T  P  E  L
                          280                        290                        300

       910        920        930        940        950        960        970        980        990
CGCGCCGACTGGATGGCCGAGCTGGAAGCGGTGCGCAGCGGCATGCTGCGCCTGCGCGAGCAATTGGCGGGCGAGTTGCGCGATCTCAGC
R  A  D  W  M  A  E  L  E  A  V  R  S  G  M  L  R  L  R  E  Q  L  A  G  E  L  R  D  L  S
                          310                        320                        330

      1000       1010       1020       1030       1040       1050       1060       1070       1080
GGTTCGGACCGTTTCGGCTTCGTGGCCGAGCATCGCGGCATGTTCTCGCGCCTGGGCGCCACGCCCGAACAGGTCAAGCGCATCAAGGAA
G  S  D  R  F  G  F  V  A  E  H  R  G  M  F  S  R  L  G  A  T  P  E  Q  V  K  R  I  K  E
                          340                        350                        360

      1090       1100       1110       1120       1130       1140       1150       1160       1170
GAGTTCGGCATCTACATGGTGGGCGATTCGCGCATCAACATCGCCGGGCTGAACGACAACACCATCCCGATCCTGGCCCGCGCTATCATC
E  F  G  I  Y  M  V  G  D  S  R  I  N  I  A  G  L  N  D  N  T  I  P  I  L  A  R  A  I  I
                          370                        380                        390

      1180       1190       1200       1210       1220       1230
GAGGTGGGGGTCTAAGCCACCGCAAGGGCGCCGGAGACGCGCCCTTTTTCTTCCACGT
E  V  G  V  *                                              R
```

Fig. 1. **Nucleotide sequence of the pdArAT gene.** The DNA fragment was amplified using the primers F (forward) and R (reverse) designed to flank the promoter and coding regions of the pdArAT gene, according to the previous data of Takagi *et al.* (*13*). Potential RNA-polymerase-binding sites and the ribosome-binding site are marked with single and double underlines, respectively. After having been ligated to pCR™II, the pdArAT-gene-containing fragment was linked with the sequence GAATTCGGCTT at the 5′ end, and AAGCCGAATTC at the 3′ end (underlines indicate the sequence recognized by *Eco*RI). The gene was excised with *Eco*RI, and ligated to the *Eco*RI site of pUC118 to construct a pdArAT expression plasmid.

agreed well with the value of M_r 42,731.58 obtained from the deduced amino acid sequence of pdArAT (Fig. 1), with a deviation (0.18%) in the range of $\pm 0.3\%$, the standard accuracy for TOF mass spectrometry. The N-terminal sequence, analyzed by a Beckman (Fullerton, CA) LF-3400 protein sequencer, was Met-Leu-Gly-Asn-Leu-Lys-Pro-Gln-Ala-, which was the same as the deduced N-terminal amino acid sequence of the enzyme (Fig. 1). These results indicated that the pdArAT gene is correctly translated as shown in Fig. 1.

The molecular weight of the native ArAT was determined to be 83 K on Sephacryl S-200 column chromatography using bovine thyroglobulin (M_r 670,000), bovine γ-globulin (M_r 158,000), chicken ovalbumin (M_r 44,000), and horse myoglobin (M_r 17,000) as standard proteins (data not shown). Thus, pdArAT has a homodimeric structure and in this respect is similar to AspATs from several sources and ecArAT. The purified pdArAT contained one PLP per

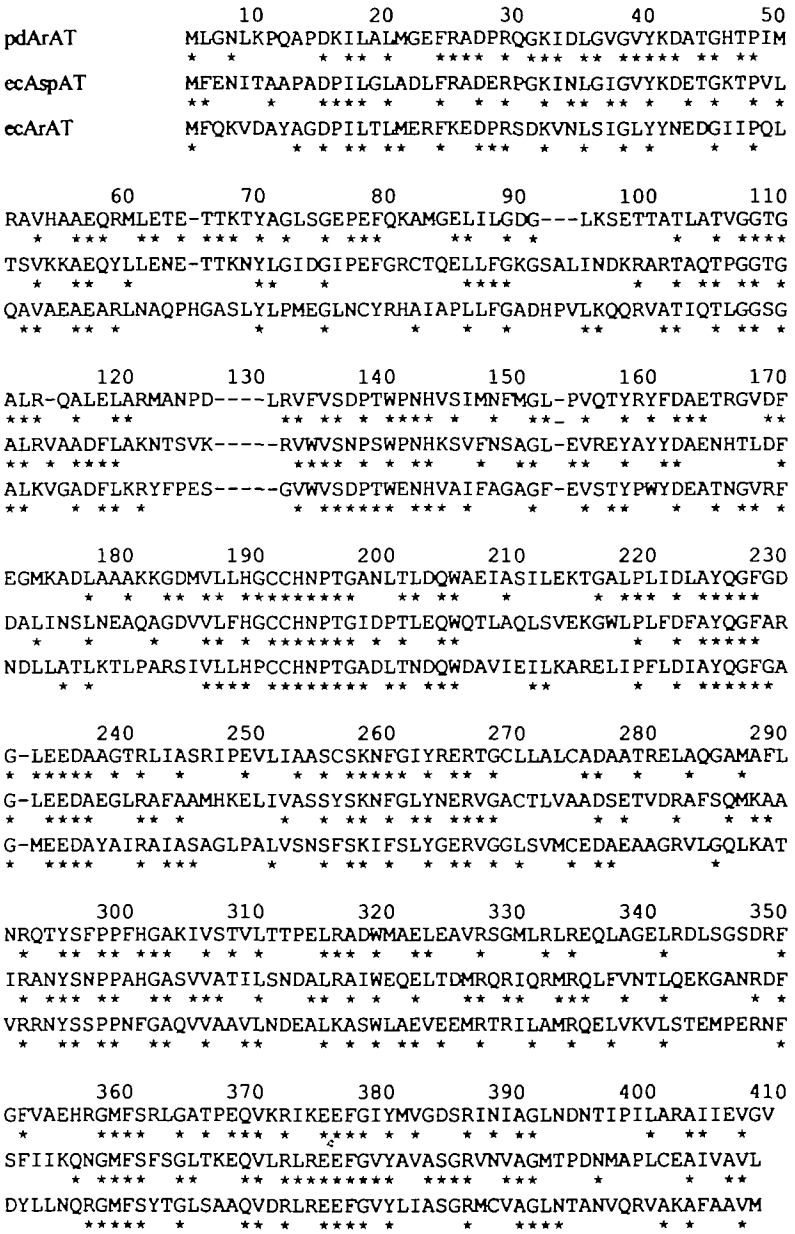

Fig. 2. **Comparison of the primary structures of pdArAT, ecArAT, and ecAspAT.** The primary structures of pdArAT (this study), ecArAT (*2, 3*) and ecAspAT (*3, 25*) were aligned using Clustal V (*36*). The residue numbers are those of pig cytosolic AspAT (*1*). Asterisks indicate the residues identical between the two flanking sequences. Asterisks shown under the ecArAT sequences are those identical between pdArAT and ecArAT sequences. The gaps common to the three sequences are due to the residue numbering based on the amino acid sequence of pig cytosolic AspAT.

subunit, which was determined by measuring the PLP content in an enzyme solution by the method of Wada and Snell (*23*, data not shown).

Comparison of the Primary Structure of pdArAT with ecArAT and ecAspAT—The primary structures of pdArAT, ecAspAT, and ecArAT can be aligned without significant deletions or insertions (Fig. 2). A database search using BLAST showed that pdArAT has high sequence homology with ecAspAT (44.7%) and ecArAT (37.6%), and to lesser extents with other subgroup I aminotransferases (*24*). The homology in the amino acid sequence between ecAspAT and ecArAT is 41.9%. Therefore, pdArAT resembles ecAspAT to the same extent as ecArAT, but pdArAT and ecArAT are slightly less homologous. Catalytically important residues identified on X-ray crystallography of ecAspAT (*6*) and AspATs from other sources (*4, 5*) were all found to be conserved at the corresponding positions in pdArAT and ecArAT. These residues include Tyr70*, forming a hydrogen bond with the phosphate group of PLP, Trp140, stacking with the pyridine ring of PLP, Asn194 and Tyr225, forming hydrogen bonds to the 3-hydroxy group of PLP, Asp222, forming a salt bridge and/or hydrogen bond to the pyridine N of PLP, Lys258, forming a Schiff base with PLP, and Arg292* and Arg386, the critical residues in binding the carboxylate groups of dicarboxylic substrates.

Absorption Spectra—The spectra of the PLP-form pdArAT at various pH values and the PMP-form pdArAT at pH 8.0 are shown in Fig. 3. pdArAT has 3 tryptophan and 8 tyrosine residues, thereby showing smaller molar absorptivity at 280 nm ($\varepsilon_M = 31{,}000\ M^{-1}\cdot cm^{-1}$ for the PLP form at pH 8.0) than ecArAT (53,000 $M^{-1}\cdot cm^{-1}$: 5 tryptophan and 15 tyrosine residues; *2, 3, 7*) and ecAspAT (47,000 $M^{-1}\cdot cm^{-1}$: 5 tryptophan and 11 tyrosine residues; *3, 17, 25*). However, the spectra over 300 nm showed striking similarities to those of ecArAT and ecAspAT (*7*). Each

PMP-form enzyme had absorption maximum at 333 nm. The PLP-form of pdArAT showed an absorption maximum at 356 nm in the alkaline region, where the ecArAT and ecAspAT absorb at 358 nm, and at 435 nm in the acidic region, where the two *E. coli* enzymes absorb at 430 nm. These pH-dependent spectral changes reflect the ionization of the aldimine nitrogen of the PLP-Lys258 Schiff base (*26*). The molar absorptivity values of pdArAT at 356 and 435 nm were plotted against pH (Fig. 4). The pK_a of the aldimine nitrogen of pdArAT was found to be 6.80 by fitting the plots to the equation

$$\varepsilon_{app} = \varepsilon_E + \frac{\varepsilon_{EH} - \varepsilon_E}{1+10^{pH-pK_a}} \quad (8)$$

where ε_E and ε_{EH} denote the molar absorptivity of the basic (E) and acidic (EH) forms of the enzyme, respectively. This pK_a value of pdArAT is similar to that of ecAspAT (pK_a = 6.85), but 0.2 pH unit higher than that of ecArAT (pK_a = 6.65) (*7*). The spectra of pdArAT in which the aldimine nitrogen is completely protonated were obtained by calculating the ε_{EH} values of Eq. 8 over the wavelength region of 300-550 nm and are shown in Fig. 3 (dashed line). The ratio of $\varepsilon_{435}/\varepsilon_{330}$ was 4.33; the value lies between the $\varepsilon_{430}/\varepsilon_{330}$ value of 3.26 for ArAT and that of 5.65 for AspAT (*7*). The absorption around 430 nm and that around 330 nm of the protonated PLP-lysine Schiff base are generally ascribed to the ketoenamine and enolimine tautomeric forms of the Schiff base, which exist in an equilibrium mixture (*27*). These alterations in tautomeric equilibrium may reflect slight changes in the strength of the hydrogen bonds of the active site residues to O3′ and N1 of PLP; such hydrogen bonds are supposed to increase the proportion of the ketoenamine form (*28*).

Reaction of ArAT with Natural and Unnatural Substrates—The reactions of pdArAT with dicarboxylic and aromatic amino/oxo acids were studied. On addition of an amino acid substrate to the PLP-form of ArAT at pH 8.0, the PLP-form absorption spectrum of the enzyme changed to that of the PMP-form, which has a peak at 333 nm (Fig. 3). In the reactions of oxo acids with the PMP-form of ArAT, the absorption maximum changed from 333 to 356 nm, demonstrating the conversion of the PMP-form to the PLP-form of the enzyme. The changes in the absorption spectrum were analyzed as described previously for the reaction of ecArAT (*7*) and ecAspAT (*17*), and the K_m and k_{cat} values for the half reactions (K_m^{half} and k_{cat}^{half}) were obtained. The values are summarized in Table I, and compared with the corresponding values of ecArAT and ecAspAT. The kinetic parameters clearly indicated that pdArAT, like ecArAT, is active toward both dicarboxylic and aromatic amino/oxo acids. The $k_{cat}^{half}/K_m^{half}$ values of pdArAT for aromatic substrates are, however, almost 10-fold smaller than those of ecArAT, mainly owing to the increased K_m^{half} values. The steady-state transamination reactions catalyzed by pdArAT of several pairs of amino-acid and oxo-acid substrates were analyzed. Double-reciprocal plots of the data fitted well to the following equation, and supported a ping-pong Bi Bi mechanism (*21, 29*).

$$\frac{v}{[E]_T} = \frac{k_{cat}^{overall}}{1+K_{m,Am}^{overall}/[Am]+K_{m,Ox}^{overall}/[Ox]} \quad (9)$$

In Eq. 9, v is the change in product concentration per unit time, and $[E]_T$ is the total enzyme concentration. The values of the parameters, $k_{cat}^{overall}$, $K_{m,Am}^{overall}$, and $K_{m,Ox}^{overall}$ are summarized in Table II. These parameters are related to the parameters of the half reaction by the following equations (*7, 17, 30*).

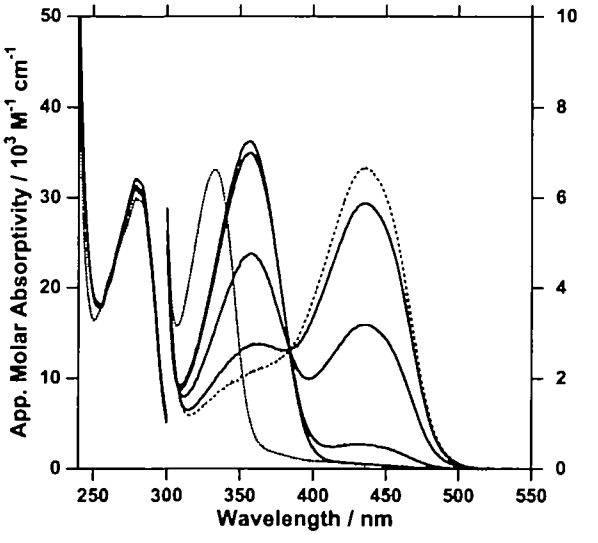

Fig. 3. **Absorption spectra of pdArAT.** The spectra were taken in a buffer solution of 50 mM PIPES-NaOH, 50 mM HEPES-NaOH, or 50 mM sodium borate, containing 0.1 M KCl, at an enzyme concentration of 7 μM, and at 25°C. Solid lines represent the spectra of the PLP-form enzymes at (from bottom to top of the 430- and 280-nm absorption bands) pH 9.2, 8.0, 6.7, and 5.9. Dotted lines represent the PMP-form enzymes at pH 8.0. The ordinate on the left shows the values for the 240–300 nm region, and the ordinate on the right for the 300–550 nm region. Dashed line shows the estimated absorption spectra of pdArAT in which the PLP-Lys258 Schiff base is in the completely protonated form. The spectrum was obtained by calculating the ε_{EH} values using the equation: $\varepsilon_{EH}\{(1+10^{(pK_a-pH_1)})\varepsilon_1-(1+10^{(pK_a-pH_2)})\varepsilon_2\}/\{10^{(pK_a-pH_1)}-10^{(pK_a-pH_2)}\}$, which was derived from Eq. 8 (*7*). In this equation, ε_1 and ε_2 represent the molar absorptivity at pH values of pH_1 and pH_2, respectively.

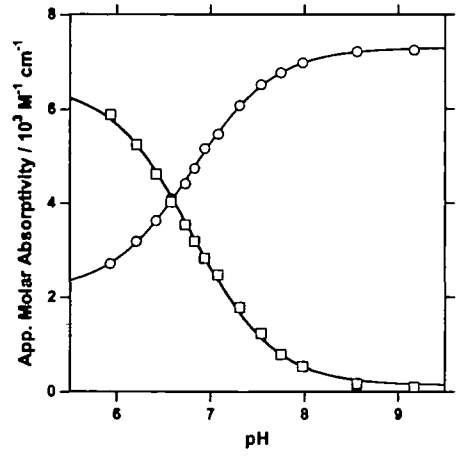

Fig. 4. **pH dependence of the molar extinction coefficients at 356 (open circles) and 435 (open squares) nm for pdArAT.** The values are at 25°C, in the presence of 50 mM buffer component(s) and 0.1 M KCl. The buffer components are the same as those used in Fig. 3. The lines represent the theoretical lines drawn by use of Eq. 8 (see text).

TABLE I. **Kinetic parameters for the half reaction of pdArAT, ecArAT, and ecAspAT toward various amino and oxo acids.** The amino acids are all L-isomers. The reactions of pdArAT with amino and oxo acids were followed by monitoring the change in absorbance at 356 nm in 50 mM HEPES-NaOH buffer containing 0.1 M KCl at 25°C, using an Applied Photophysics SX.17MV stopped-flow spectrophotometer. K_m, k_{cat}, and k_{cat}/K_m values are those for half transamination reactions. K_m (mM), k_{cat} (s^{-1}), and k_{cat}/K_m ($M^{-1} \cdot s^{-1}$).

		pdArAT	ecArAT[a]	ecAspAT[b]
(E_{PLP} + amino acid)				
Phenylalanine	K_m	4.6 ± 0.2	1.0	*ns*[c]
	k_{cat}	990 ± 8	1,200	*ns*
	k_{cat}/K_m	220,000	1,200,000	200
Tyrosine	K_m	2.9 ± 0.5	0.83	*ns*
	k_{cat}	1,100 ±140	500	*ns*
	k_{cat}/K_m	390,000	600,000	400
Tryptophan	K_m	8.0 ± 0.6	0.68	34
	k_{cat}	550 ± 7	350	30
	k_{cat}/K_m	69,000	510,000	880
Aspartate	K_m	1.6 ± 0.2	5.0	4.5
	k_{cat}	320 ± 20	290	550
	k_{cat}/K_m	200,000	58,000	120,000
Glutamate	K_m	95 ± 3	120	38
	k_{cat}	2,000 ± 40	1,200	700
	k_{cat}/K_m	21,000	10,000	18,000
(E_{PMP} + oxo acid)				
Phenylpyruvate	K_m	0.24 ± 0.01	0.025	6.7
	k_{cat}	1,000 ± 10	490	56
	k_{cat}/K_m	4,200,000	20,000,000	8,400
Hydroxyphenyl-pyruvate	K_m	0.30 ± 0.02	0.040	3.3
	k_{cat}	1,400 ± 40	650	50
	k_{cat}/K_m	4,700,000	16,000,000	15,000
Indolepyruvate	K_m	0.33 ± 0.03	0.057	3.0
	k_{cat}	540 ± 13	560	54
	k_{cat}/K_m	1,600,000	9,800,000	18,000
Oxalacetate	K_m	0.035± 0.003	0.082	0.035
	k_{cat}	1,200 ± 20	830	800
	k_{cat}/K_m	34,000,000	10,000,000	23,000,000
2-Oxoglutarate	K_m	2.3 ± 0.22	1.67	1.3
	k_{cat}	1,700 ± 80	360	600
	k_{cat}/K_m	740,000	220,000	18,000

[a]Taken from Hayashi *et al.* (7). [b]Taken from Kuramitsu *et al.* (17). [c]*ns*: No saturation with respect to substrate concentration was observed.

TABLE II. **Kinetic parameters of the pdArAT-catalyzed overall reactions.** The steady-state kinetic parameters for the ping-pong Bi Bi reactions are shown. The rates of pdArAT-catalyzed transamination reactions from aspartate to aromatic 2-oxo acids under steady-state conditions were measured using malate dehydrogenase (MDH)-coupling assay in 50 mM HEPES-NaOH buffer, pH 8.0, containing 0.1 M KCl at 25°C (see "MATERIALS AND METHODS"). The values in parenthesis are those obtained using the kinetic parameters for the half reactions (Table I) and Eqs. 10-12.

Substrate pair	$K_m^{overall}$ (mM)	$k_{cat}^{overall}$ (s^{-1})
Aspartate	1.8 (1.4)	170 (270)
2-Oxoglutarate	0.59 (0.36)	
Aspartate	1.9 (1.2)	130 (240)
3-Phenylpyruvate	0.083 (0.058)	
Aspartate	1.9 (1.2)	140 (260)
3-(4-Hydroxy-phenyl)pyruvate	0.059 (0.056)	
Tryptophan	1.4 (1.0)	100 (200)
2-Oxoglutarate	0.14 (0.11)	

$$k_{cat}^{overall} = \frac{k_{cat,Am}^{half} k_{cat,Ox}^{half}}{k_{cat,Am}^{half} + k_{cat,Ox}^{half}} \quad (10)$$

$$K_{m,Am}^{overall} = \frac{k_{cat,Ox}^{half}}{k_{cat,Am}^{half} + k_{cat,Ox}^{half}} K_{m,Am}^{half} \quad (11)$$

$$K_{m,Ox}^{overall} = \frac{k_{cat,Am}^{half}}{k_{cat,Am}^{half} + k_{cat,Ox}^{half}} K_{m,Ox}^{half} \quad (12)$$

Then the values of the overall-reaction parameters were calculated using the half-reaction parameters, and the values are listed in Table II in parenthesis. That the calculated values were found to be in good agreement with the corresponding observed values shows that the values in Table I reflect the true half reactions of the overall trans-

TABLE III. **The $k_{cat}^{half}/K_m^{half}$ values for the half reactions of amino acids with the PLP form of pdArAT.** The reaction was followed by monitoring the decrease in absorbance at 356 nm in the same way as described in Table I, in 50 mM HEPES-NaOH buffer, pH 8.0, containing 0.1 M KCl at 25°C.

	pdArAT	ecArAT[b]	ecAspAT[c]
2-Aminooctanoate[a]	7,800 ±480	610,000	4.0
2-Aminoheptanoate[a]	1,200 ± 20	81,000	23
Norleucine	280 ± 4	3,400	4.9
Norvaline	62 ± 1	140	1.1
2-Aminobutyrate[a]	7.5 ± 0.1	10.5	0.45
Alanine	3.7 ± 0.1	2.0	0.77
Leucine	110 ± 0.8	380	2.4
Methionine	510 ± 4	920	22
Histidine	340	670	13
Asparagine	11	18	1.4
Glutamine	3.5	2.5	0.74
Serine	0.59 ± 0.01	0.098	0.050
Threonine	0.004± 0.0005	0.074	0.010
Isoleucine	0.013± 0.001	<0.001	<0.001
Valine	0.026± 0.00003	0.17	<0.001
Lysine	0.28 ± 0.0005	0.48	0.010
Arginine	0.15 ± 0.001	0.51	0.010

[a]DL-form of amino acid was used. The values are for L-form. [b]Taken from Hayashi *et al.* (7). [c]Taken from Kuramitsu *et al.* (17).

amination reaction.

The reactions of other amino acids, including natural and unnatural amino acids, with the PLP form of the enzyme were followed similarly, and the kinetic parameters for the half reaction were obtained (Table III). Saturation of k_{app} with [S] was not apparent for these amino acids, probably due to high K_m^{half} values relative to the concentration of amino acids used, and only the $k_{cat}^{half}/K_m^{half}$ values were obtained. The catalytic efficiency expressed by $k_{cat}^{half}/K_m^{half}$ showed that amino acids with bulky side chains, including aromatic substrates, are efficient substrates for pdArAT, as in the case of ecArAT and ecAspAT. Furthermore, valine and isoleucine, both of which have a branching at C^β, were poor substrates for both ArATs and ecAspAT; this has been considered to be due to the steric hindrance between the group at C^β and Tyr70* in ecArAT (*7*). Therefore, there is similar tendency in substrate specificity between pdArAT, ecArAT, and ecAspAT, suggesting the importance of hydrophobic interaction between substrate side chain and enzyme and the shape of the substrate side chain with no branching at C^β for binding of neutral amino acids to the active site of the enzyme.

Because the energy of the hydrophobic interaction between substrate and enzyme is dependent on the surface area of the substrate side chain, it is necessary to take into account the side chain surface area in thermodynamic comparison of the reactions with different substrates. Therefore, we plotted the activation free energy ($\Delta G_T^\ddagger$) values for the half reaction of aromatic amino acids and aliphatic amino acids against the side chain surface area of the substrates (Fig. 5). For each enzyme, there was a tendency for the $\Delta G_T^\ddagger$ value to decrease with increasing side-chain surface area, and this tendency was more prominent in pdArAT and ecArAT than ecAspAT. This suggests a stronger hydrophobic interaction in the two ArATs than that in ecAspAT. For ecArAT, the $\Delta G_T^\ddagger$ values for phenylalanine, tyrosine, 2-aminoheptanoate, and 2-aminooctanoate, which have similar side-chain surface areas, were essentially alike (Fig. 5, panel B). Therefore, in the case of ecArAT, substrate specificity is for the most part determined by the surface area, and not by the shape, of the substrate side chain. On the other hand, for pdArAT, the values for phenylalanine and tyrosine are more than 10 $kJ \cdot mol^{-1}$ lower than the values for 2-aminoheptanoate and 2-aminooctanoate (Fig. 5, panel A). This indicates that, in the transition-state structure, aromatic rings bind to the active site of pdArAT far more strongly than aliphatic groups with similar side-chain surface area. Therefore we can consider that the binding site for the neutral side chain of substrates of pdArAT has a shape that matches well with the phenyl ring of phenylalanine or the hydroxyphenyl ring of tyrosine. In ecArAT, the site that accepts the aromatic ring of aromatic substrates has been shown to be near Arg292*, the residue that binds the distal carboxylate group of dicarboxylic substrates (*10*). Therefore, it is important to know the aromatic-ring-accepting site in pdArAT, in order to discuss the difference in preference for aromatic side chain between the two ArATs. We analyzed this using substrate analogs and 3-hydroxylated quasisubstrates (*7, 10*).

Reaction with Substrate Analogs and Quasisubstrates—Addition of dicarboxylic acids such as maleate, succinate, and glutarate to ecAspAT and ecArAT shifted the absorption band of the enzymes at 358 to 430 nm (*31, 32*). In the case of ecArAT, aromatic carboxylic acids, 3-phenylpropionate, 3-(4-hydroxyphenyl)propionate, and 3-indolepropionate, which are structural analogs for phenylalanine, tyrosine, and tryptophan, respectively, also bound to the enzyme, giving rise to a similar shift of the position of the absorption band from 358 to 430 nm (*7, 32*). These spectral shifts are due to a 1.5–2-units increase in the pK_a value of the aldimine formed between PLP and Lys258 caused by the negative charge of the carboxylate groups (*31, 32*). These dicarboxylates and aromatic carboxylates gave similar absorption changes when they bound to pdArAT, with K_d values comparable to those in the case of ecArAT

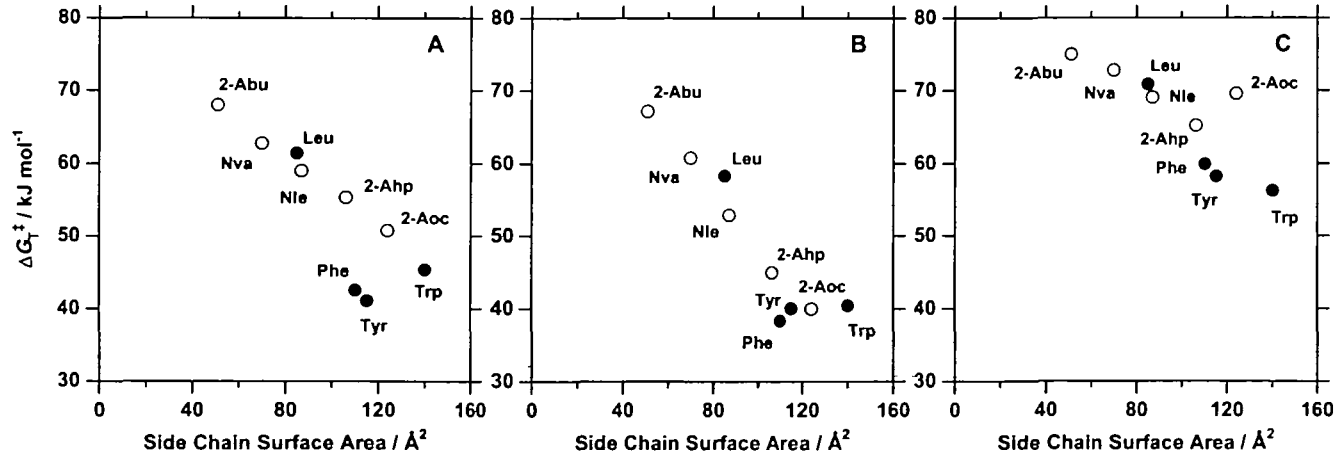

Fig. 5. **Activation free energy ($\Delta G_T^\ddagger$) values for the reaction of pdArAT (A), ecArAT (B), or ecAspAT (C) with neutral amino acids plotted against the surface area of the amino acid side chains.** pH 8.0, 25°C. The letters beside the plots denote amino acids: 2-Abu, 2-amino-butyrate; Nva, norvaline; Leu, leucine; Nle, norleucine; 2-Ahp, 2- aminoheptanoate; 2-Aoc, 2-aminooctanoate; Phe, phenylalanine; Tyr, tyrosine; Trp, tryptophan. Straight-chain aliphatic amino acids are shown by open circles, and other amino acids byclosed circles. The free energy difference ($\Delta G_T^\ddagger$) between the transition state for the half transamination reaction ($ES^\ddagger$) and unbound enzyme plus substrate (E+S) was calculated from the $k_{cat}^{half}/K_m^{half}$ values listed in Tables I and III using the equation $\Delta G_T^\ddagger = RT[\ln(k_B T/h) - \ln(k_{cat}^{half}/K_m^{half})]$ (*37*). Side chain surface area for each amino acid was calculated using Quanta (version 4.0, Molecular Simulations, Waltham, MA) for the CHARMm-minimized conformation.

(Table IV). We tested fumarate and *trans*-cinnamate, both of which have a double bond between C(2) and C(3) like maleate, but in a *trans* configuration. In contrast to maleate, which has a *cis* configuration, these *trans* compounds essentially did not bind to pdArAT or ecArAT. The finding that *trans*-cinnamate essentially does not bind to either of the two ArATs is consistent with the idea that the aromatic rings of aromatic substrates and analogs share the same binding site as the carboxylate group of dicarboxylic substrates and analogs.

The reactions of pdArAT with L-*erythro*-3-hydroxyaspartate and L-*erythro*-3-phenylserine were studied on a stopped-flow spectrophotometer equipped with a photodiode array detector. Like the reactions with ecAspAT (3-hydroxyaspartate only; *33*) and ecArAT (*10*), the reactions of the two 3-hydroxy amino acids with pdArAT proceeded in a biphasic manner; the first phase corresponds to the formation of the quinonoid intermediate (Q) from the external aldimine (ES; a Schiff base between PLP and the quasisubstrate in the active site) and the second phase corresponds to the slow decay of the quinonoid signal due to slow equilibration of the quinonoid intermediate and the carbinolamine intermediate. The spectrum just after the first phase of the biphasic spectral change is that of an equilibrium mixture of E, ES, and Q. Extrapolation to an infinite concentration of the 3-hydroxy amino acid gave the spectrum of an equilibrium mixture of ES and Q (Fig. 6, curve 3 in each panel). The spectrum of the ES/Q equilibrium mixture of the L-*erythro*-3-hydroxyaspartate-pdArAT complex and that of the L-*erythro*-3-phenylserine-pdArAT complex showed the absorption maximum at 493 nm and at 497 nm, with apparent molar absorptivity of 29,000 and 10,000 $M^{-1} \cdot cm^{-1}$, respectively. This indicates that the 3-hydroxy group of L-*erythro*-3-phenylserine stabilizes and accumulates the quinonoid intermediate in the same way as the 3-hydroxy group of L-*erythro*-3-hydroxyaspartate in pdArAT, although the equilibrium between the ES and Q is shifted toward ES in the L-*erythro*-3-phenylserine-pdArAT complex ($[Q]_{eq}/[ES]_{eq} = 0.42$) and toward Q in the L-*erythro*-3-hydroxyaspartate-pdArAT complex ($[Q]_{eq}/[ES]_{eq} = 7.1$). The *threo* isomers of these 3-hydroxy amino acids are substrates for pdArAT without producing the quinonoid absorption, as has been observed for the reaction of these isomers with ecArAT (data not shown). Therefore, although there is a discrepancy in the $[Q]_{eq}/[ES]_{eq}$ value, the identification of the quinonoid intermediate stabilized by the 3-hydroxy group in the *erythro* configuration in both 3-hydroxy amino acids indicates superimposable conformations of the two quasisubstrates.

TABLE IV. **Binding of substrate analogs to pdArAT.** The extent of the substrate analog binding to pdArAT was measured by monitoring the spectral transition of the PLP-Lys258 absorption at 25°C, in 50 mM HEPES-NaOH buffer, pH 8.0, containing 0.1 M KCl. Standard deviation values are shown in parenthesis.

	pdArAT K_d (mM)	ecArAT[b] K_d (mM)	ecAspAT[c] K_d (mM)
3-Phenylpropionate	3.9 (0.3)	8.5	*nc*[d]
trans-Cinnamate	*nc*	*nc*	*nc*
3-(4-Hydroxyphenyl)propionate	1.1 (0.003)	7.0	*nc*
Succinate	24.9 (0.4)		74
Fumarate	*nc*	*nc*	*nc*
Maleate	2.9 (0.1)	6.6	10
2-Me-aspartate[a]	2.6 (0.26)	9.2	2.6
2-Me-tryptophan[a]	*nc*	0.62	*nc*
2-Me-tyrosine[a]	*nc*	1.1	*nc*
2-Me-phenylalanine[a]	*nc*	5.3	*nc*

[a]DL-form was used. The K_d values are for L-form. [b]Taken from Hayashi *et al.* (*7*). [c]Taken from Kuramitsu *et al.* (*17*). [d]*nc*: No apparent spectral changes were observed at 50 mM [3-phenylpropionate, *trans*-cinnamate, 3-(4-hydroxyphenyl)propionate, and fumarate], 25 mM (2-methyltryptophan and 2-methylphenylalanine), or 1.25 mM (2-methyltyrosine).

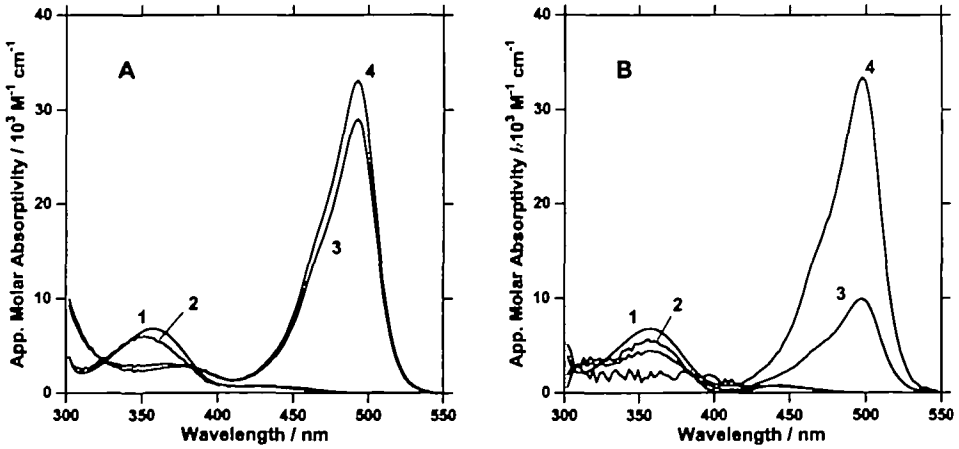

Fig. 6. **Absorption spectra of pdArAT during the reaction with 3-hydroxy amino acids.** The spectra were taken in 50 mM HEPES-NaOH buffer, pH 8.0, containing 0.1 M KCl, at 25°C. (A) Reaction with L-*erythro*-3-hydroxyaspartate. (B) Reaction with L-*erythro*-3-phenylserine. The reaction was followed in an Applied Photophysics SX.17MV stopped-flow spectrophotometer equipped with a photodiode array detector. The data were taken at 117 wavelengths with equal intervals between 302.4 and 544.2 nm, and were processed according to the reaction scheme E+S⇌ES⇌Q, as described previously for the reaction of ecAspAT with L-*erythro*-3-hydroxyaspartate (*33*). In each panel, curve 1 represents the spectrum in the absence of the 3-hydroxy amino acid. Curve 2 and curve 3 show the spectra just after the encounter of E (enzyme) and S (3-hydroxy amino acid), and after the exponential increase in the absorbance at 500 nm, each extrapolated to an infinite concentration of the 3-hydroxy amino acid. Thus, curve 2 represents the spectrum of ES, and curve 3 the equilibrium mixture of ES (the Michaelis complex and/or the external aldimine, *i.e.*, the substrate amino acid-PLP Schiff base) and Q (the quinonoid intermediate). The spectrum of Q, represented by curve 4, was calculated using the rate constant for the step ES⇌Q, obtained in this study according to the method described previously (*33*). Owing to the relatively strong absorption of L-*erythro*-3-phenylserine in the UV region, the concentration of L-*erythro*-3-phenylserine used to measure the spectra was less than 20 mM, although the binding of the amino acid to pdArAT is weak with the K_s value of 44.2 mM. This enhanced the spectral noise, especially at wavelength shorter than 400 nm, where the S/N ratio is low, during the extrapolation process (panel B).

strates in the active site of pdArAT, and suggests the presence of a common binding site of the aromatic ring and the carboxylate group (*10*).

Comparison of pdArAT and ecArAT—The above results show that the site of pdArAT that accepts the aromatic side chains of substrates is close to the region that accepts the distal carboxylate group of dicarboxylic substrates. This dual substrate-recognition mechanism is essentially identical with that of ecArAT (*7, 10*). However, pdArAT has high specificity toward aromatic amino acids relative to the other neutral amino acids, and this is a unique feature of this enzyme which distinguishes it from ecArAT (Tables I and III and Fig. 5). Therefore, although the position of the aromatic-binding pocket in the enzyme molecule appears to be the same, there seems to be some difference in the shape of the pocket between the two ArATs.

That the substrate-side-chain-binding pocket of pdArAT binds the phenyl and hydroxyphenyl groups more strongly than the aliphatic groups suggests that the interaction of these aromatic rings with the pocket is strict and little accommodation can be made to different shape or position of the side chains of substrates. In accordance with this notion, some of the data on the reactions of 3-hydroxylated amino acids with pdArAT, and the binding of 2-methyl amino acids can be interpreted as follows. The incorporation of a hydroxy group, or a methyl group into substrate amino acids probably causes steric hindrance of these groups with the residues in the enzyme active site. Then, the position and conformation of the substrate, when bound to the enzyme, must be slightly changed in such a way that the substituted groups do not produce constraints with the active site. In the case of aspartate, having a smaller side chain relative to that of phenylalanine or tyrosine, this accommodation may be possible, but in the case of phenylalanine and tyrosine, the strict requirements for interaction of these aromatic rings with the substrate-side-chain-binding pocket of pdArAT would oppose such accommodation. That the quinonoid intermediate of the L-*erythro*-3-phenylserine-pdArAT is more unstable than that of the L-*erythro*-3-hydroxyaspartate-pdArAT complexes, and that the 2-methylphenylalanine and 2-methyltyrosine essentially do not bind to pdArAT, whereas 2-methylaspartate does bind to the enzyme, can be interpreted in terms of this mechanism. On the other hand, the previous finding (*10*) that the quinonoid intermediate of L-*erythro*-3-phenylserine-ecArAT is as stable as that of the L-*erythro*-3-hydroxyaspartate-ecArAT complex, and that 2-methylphenylalanine and 2-methyltyrosine bind to ecArAT as well as 2-methylaspartate (*7*), are considered to reflect the nature of the substrate-side-chain-binding pocket of ecArAT that can allow some adjustments of the position and conformation of the 2- or 3-substituted aromatic amino acids. That phenylpropionate and hydroxyphenylpropionate can bind to pdArAT as well as to ecArAT is considered to be because these analogs have no substituted groups on their skeletons that may cause steric hindrance with the enzyme active site.

Both ArATs show almost equal sequence homology with ecAspAT, the enzyme which is active preferentially toward dicarboxylic substrates. Therefore, these three sequences were compared in the light of their relevance to substrate specificity. As the residues that directly interact with the substrates and the coenzymes form the "core" of the active site and are invariant among the three sequences (Fig. 2), residues that are adjacent to them and are varied among the three sequences are of interest. Among these residues, Leu39, Tyr41, Ile47, Leu69*, Ser109, and Ser297* have been shown by Onuffer and Kirsch (*34*) to be critical for the recognition of aromatic substrates in ecArAT; changing the corresponding 6 residues of ecAspAT (Val39, Lys41, Thr47, Asn69*, Thr109, and Asn297*) to the ecArAT residues greatly increased the activity of ecAspAT toward aromatic substrates. X-ray crystallography of the hexamutant enzyme complexed with phenylpropionate showed that the aromatic ring of phenylpropionate is located at the position that is occupied by the carboxylate group of maleate interacting with Arg292* in the enzyme-maleate complex (*35*). The hexamutant enzyme enables this mode of aromatic binding by reorienting the side chain of Arg292* toward the solvent. Malashkevich *et al.* (*35*) considered that the driving force that rotates the side chain of Arg292* out of the active site is the increased hydrophobicity of the active site caused by the 4 mutations, Val39Leu, Lys41Tyr, Thr47Ile, and Asn69*Leu. In addition, they considered that the aromatic-side-chain-binding pocket is formed by the Asn297*Ser and Thr109Ser mutations; the reduction in size of the side chain at 297* alters the position of the water molecule hydrogen-bonded to the 297* side chain (asparagine in ecAspAT) so that it does not undergo unfavorable interaction with the aromatic ring of substrates, and the replacement at 109 has a fine-tuning effect to adjust the position of the indole ring of Trp140 so that the substrate aromatic ring can be accommodated. However, the residues 39, 41, 47, and 109 are identical between pdArAT and ecAspAT, and the residue 69* is threonine, which is more hydrophilic than the leucine residue of ecArAT. Apparently, the residues 39, 41, 47, and 69* do not increase the hydrophobicity of the pdArAT active site, as compared with the corresponding residues in ecArAT. This suggests that the aromatic-recognition mechanism that has been proposed for the hexamutant ecAspAT and extended to ecArAT may not be applicable to the aromatic-substrate recognition of pdArAT. X-ray crystallographic analysis of the aromatic carboxylate complex of pdArAT may unravel a new type of aromatic-substrate-accommodating mechanism, which is different from that of the hexamutant ecAspAT or ecArAT. A study on this is under way in our laboratory.

We thank Dr. Masahiko Kishikawa and Prof. Akira Shimizu, Department of Clinical Pathology, Osaka Medical College, for TOF-mass spectroscopic analysis.

REFERENCES

1. Doonan, S., Doonan, H.J., Hanford, R., Vernon, C.A., Walker, J.M., da Airold, L.P., Bossa, F., Barra, D., Carloni, M., Fasella, P., and Riva, F. (1975) The primary structure of aspartate aminotransferase from pig heart muscle. Digestion with a proteinase having specificity for lysine residues. *Biochem. J.* **149**, 497-506
2. Kuramitsu, S., Inoue, K., Ogawa, T., Ogawa, H., and Kagamiyama, H. (1985) Aromatic amino acid aminotransferase of *Escherichia coli*: nucleotide sequence of the *tyrB* gene. *Biochem. Biophys. Res. Commun.* **133**, 134-139
3. Fotheringham, I.G., Dacey, S.A., Taylor, P.P., Smith, T.J., Hunter, M.G., Finlay, M.E., Primrose, S.B., Parker, D.M., and

Edwards, R.M. (1986) The cloning and sequence analysis of the *aspC* and *tyrB* genes from *Escherichia coli* K12. Comparison of the primary structures of the aspartate aminotransferase and aromatic aminotransferase of *E. coli* with those of the pig aspartate aminotransferase isoenzymes. *Biochem. J.* **234**, 593-604

4. Arnone, A., Rogers, P.H., Hyde, C.C., Briley, P.D., Metzler, C.M., and Metzler, D.E. (1985) Pig cytosolic aspartate aminotransferase: The structures of the internal aldimine, external aldimine, and ketimine and of the β-subform in *Transaminases* (Christen, P. and Metzler, D.E., eds.) pp. 138-154, John Wiley and Sons, New York
5. Jansonius, J.N., Eichele, G., Ford, G.C., Picot, D., Thaller, C., and Vincent, M. (1985) Spatial structure of mitochondrial aspartate aminotransferase in *Transaminases* (Christen, P. and Metzler, D.E., eds.) pp. 109-137, John Wiley & Sons, New York
6. Okamoto, A., Higuchi, T., Hirotsu, K., Kuramitsu, S., and Kagamiyama, H. (1994) X-ray crystallographic study of pyridoxal 5′-phosphate-type aspartate aminotransferases from *Escherichia coli* in open and closed form. *J. Biochem.* **116**, 95-107
7. Hayashi, H., Inoue, K., Nagata, T., Kuramitsu, S., and Kagamiyama, H. (1993) *Escherichia coli* aromatic amino acid aminotransferase: characterization and comparison with aspartate aminotransferase. *Biochemistry* **32**, 12229-12239
8. Powell, J.T. and Morrison, J.F. (1978) The purification and properties of the aspartate aminotransferase and aromatic-amino-acid aminotransferase from *Escherichia coli*. *Eur. J. Biochem.* **87**, 391-400
9. Köhler, E., Seville, M., Jäger, J., Fotheringham, I., Hunter, M., Edwards, M., Jansonius, J.N., and Kirschner, K. (1994) Significant improvement to the catalytic properties of aspartate aminotransferase: Role of hydrophobic and charged residues in the substrate binding pocket. *Biochemistry* **33**, 90-97
10. Hayashi, H., Inoue, K., Mizuguchi, H., and Kagamiyama, H. (1996) Analysis of the substrate-recognition mode of aromatic amino acid aminotransferase by combined use of quasisubstrates and site-directed mutagenesis: Systematic hydroxy-group addition/deletion studies to probe the enzyme-substrate interactions. *Biochemistry* **35**, 6754-6761
11. Onuffer, J.J., Ton, B.T., Klement, I., and Kirsch, J.F. (1995) The use of natural and unnatural amino acid substrates to define the substrate specificity differences of *Escherichia coli* aspartate and tyrosine aminotransferases. *Protein Sci.* **4**, 1743-1749
12. Nakai, Y., Hayashi, H., and Kagamiyama, H. (1996) Cloning and characterization of the *tyrB* gene from *Salmonella typhimurium*. *Biochim. Biophys. Acta* **1308**, 189-192
13. Takagi, T., Taniguchi, T., Yamamoto, Y., and Shibatani, T. (1991) Molecular cloning of the L-phenylalanine transaminase gene from *Paracoccus denitrificans* in *Escherichia coli* K-12. *Biotechnol. Appl. Biochem.* **13**, 112-119
14. Jones, J.H. (1979) α-Amino-ω-hydroxy acids in *Comprehensive Organic Chemistry* (Barton, D.H.R. and Ollis, W.D., eds.) Vol. 2 (Sutherland, I.O., ed.) pp. 2589-2643, Pergamon Press, Oxford, UK
15. Jenkins, W.T. (1979) Preparation of the diastereoisomers of β-hydroxy-L-aspartate with pig heart aspartate aminotransferase. *Anal. Biochem.* **93**, 134-138
16. Albertson, N.F. (1946) The synthesis of amino acids from ethyl acetamidomalonate and ethyl acetamidocyanoacetate. III. The use of primary halides. *J. Am. Chem. Soc.* **69**, 450-453
17. Kuramitsu, S., Hiromi, K., Hayashi, H., Morino, Y., and Kagamiyama, H. (1990) Pre-steady-state kinetics of *Escherichia coli* aspartate aminotransferase catalyzed reactions and thermodynamic aspects of its substrate specificity. *Biochemistry* **29**, 5469-5476
18. Ausubel, F.M., Brent, R., Kingston, R.E., Moore, D.D., Seidman, J.G., Smith, J.A., and Struhl, K. (1994) *Current Protocols in Molecular Biology* suppl. 27, unit 2.4, John Wiley & Sons, New York
19. Inoue, K., Kuramitsu, S., Aki, K., Watanabe, Y., Takagi, T., Nishigai, M., Ikai, A., and Kagamiyama, H. (1988) Branched-chain amino acid aminotransferase of *Escherichia coli*: Overproduction and properties. *J. Biochem.* **104**, 777-784
20. Yano, T., Kuramitsu, S., Tanase, S., Morino, Y., Hiromi, K., and Kagamiyama, H. (1991) The role of His143 in the catalytic mechanism of *Escherichia coli* aspartate aminotransferase. *J. Biol. Chem.* **266**, 6079-6085
21. Kiick, D.M. and Cook, P.F. (1983) pH studies toward the elucidation of the auxiliary catalyst for pig heart aspartate aminotransferase. *Biochemistry* **22**, 375-382
22. Jensen, R.A. and Gu, W. (1996) Evolutionary recruitment of biochemically specialized subdivisions of family I within the protein superfamily of aminotransferases. *J. Bacteriol.* **178**, 2161-2171
23. Wada, H. and Snell, E.E. (1961) The enzymatic oxidation of pyridoxine and pyridoxamine phosphates. *J. Biol. Chem.* **236**, 2089-2095
24. Mehta, P.K., Hale, T.I., and Christen, P. (1993) Aminotransferases: demonstration of homology and division into evolutionary subgroups. *Eur. J. Biochem.* **214**, 549-561
25. Kuramitsu, S., Okuno, S., Ogawa, T., Ogawa, H., and Kagamiyama, H. (1985) Aspartate aminotransferase of *Escherichia coli*: nucleotide sequence of the *aspC* gene. *J. Biochem.* **97**, 1259-1262
26. Kallen, R.G., Korpela, T., Martell, A.E., Matsushima, Y., Metzler, C.M., Metzler, D.E., Morozov, Yu.V., Ralston, I.M., Savin, F.A., Torchinsky, Yu.M., and Ueno, H. (1985) Chemical and spectroscopic properties of pyridoxal and pyridoxamine phosphates in *Transaminases* (Christen, P. and Metzler, D.E., eds.) pp. 37-108, John Wiley & Sons, New York
27. Johnson, G.F., Tu, J.-I., Shonka Bartlett, M.L., and Graves, D.J. (1970) Physical-chemical studies on the pyridoxal phosphate binding site in sodium borohydride-reduced and native phosphorylase. *J. Biol. Chem.* **245**, 5560-5568
28. Metzler, C.M., Viswanath, R., and Metzler, D.E. (1991) Equilibria and absorption spectra of tryptophanase. *J. Biol. Chem.* **266**, 9374-9381
29. Velick, S.F. and Vavra, J. (1962) A kinetic and equilibrium analysis of glutamic oxaloacetate transaminase mechanism. *J. Biol. Chem.* **237**, 2109-2122
30. Fasella, P. and Hammes, G.G. (1967) A temperature jump study of aspartate aminotransferase. A reinvestigation. *Biochemistry* **6**, 1798-1804
31. Jenkins, W.T. and D'Ari, L. (1966) Glutamic-aspartic transaminase. X. Mechanism and order of formation of the enzyme-substrate carboxylate bonds. *J. Biol. Chem.* **241**, 5667-5674
32. Iwasaki, M., Hayashi, H., and Kagamiyama, H. (1994) Protonation state of the active-site Schiff base of aromatic amino acid aminotransferase: modulation by binding of ligands and implications for its role in catalysis. *J. Biochem.* **115**, 156-161
33. Hayashi, H. and Kagamiyama, H. (1995) Reaction of aspartate aminotransferase with L-*erythro*-3-hydroxyaspartate: Involvement of Tyr70 in stabilization of the catalytic intermediates. *Biochemistry* **34**, 9413-9423
34. Onuffer, J.J. and Kirsch, J.F. (1995) Redesign of the substrate specificity of *Escherichia coli* aspartate aminotransferase to that of *Escherichia coli* tyrosine aminotransferase by homology modeling and site-directed mutagenesis. *Protein Sci.* **4**, 1750-1757
35. Malashkevich, V.N., Onuffer, J.J., Kirsch, J.F., and Jansonius, J.N. (1995) Alternating arginine-modulated substrate specificity in an engineered tyrosine aminotransferase. *Nature Struct. Biol.* **2**, 548-553
36. Higgins, D.G. (1994) CLUSTAL V: multiple alignment of DNA and protein sequences. *Methods Mol. Biol.* **25**, 307-318
37. Fersht, A. (1985) *Enzyme Structure and Mechanism*, W.H. Freeman and Company, New York